Fixed bed column studies for decontamination of acidic mineral effluent using porous Fly Ash-Basic Oxygen Furnace slag based geopolymers

N.T. Sithole[1], F Ntuli[1], F. Okonta[2]

*[1] University of Johannesburg, Department of Chemical Engineering, P.O. Box 17011, Doornfontein 2088, South Africa, email address: fntuli@uj.ac.za * corresponding author email address:nastassias@uj.ac.za*
[2]Department of Civil Engineering Science, University of Johannesburg, P O Box 524, Auckland Park, 2006, Johannesburg, South Africa, email address:fnokonta@uj.ac.za

Abstract

This paper presents column studies conducted to evaluate and assess the potential use of Fly Ash (FA)- Basic Oxygen Furnace Slag (BOFS) based geopolymers to remove metals, sulphates and acidity from Acid Mine Drainage (AMD). Geopolymers were prepared using NaOH, Fly ash (FA) was used as source of silica additive to supplement BOFS. The blending ratio was fixed to 10% FA and the S/L ratio was kept 20 %. The H_2O_2 was used as a blowing agent to increase the porosity of the FA/BOFS based geopolymer at four different percentages (1.5 %, 1 %, 0.5 % and 0 %). The four different geopolymers with distinct porosities were employed in different columns respectively. It was found that over 99% removal efficiency of metals and sulphates was achieved in the first 60 days of column studies. The dissolution of $Ca(OH)_2$ was the main constituent responsible for the removal of acidity in AMD. Characterization revealed that precipitation was the main mechanism for removal of metals. Gypsum was the main byproduct formed with precipitated metals presented by goethite, spertite and manganite.

1. Introduction

Acid mine drainage (AMD) contains iron as a major metal with variable concentrations of aluminum, manganese, zinc, nickel, copper and other metals which are discharged into various water bodies due to industrial activities such as mining activities, metal reduction and smelting (Wan Ngah 2008; Dobchuk 2015). AMD is toxic to human health and the environment as a result of water and soil pollution (Aguiar 2015). The aforementioned toxic metals can cause various diseases and disorders in human, animals, and aquatic life. The envisaged increase of AMD production in the mining and mineral processing sectors necessitates the need to remove toxic heavy metals before the effluent is discharged into water streams. The disposal of toxic heavy metals or by-products has become more difficult and expensive because of the increasing

stringent environmental regulations (Ahmed et al., 2016) However, in actual practice such regulations are often violated and as a result the environment gets affected (Abdi et al., 2011).

Currently the mining industry is faced with the challenge of acidic effluents specifically AMD. If AMD is not treated, it could potentially pollute the water supply, which will impact industries, such as agriculture and manufacturing (Venmyn 2013). Considering the environmental and ecological threats this poses, it is of paramount importance to remove toxic heavy metals from AMD.

There are number of technologies that are used nationally and internationally to remove heavy metals from AMD. These methods include; precipitation, electrolytic membranes, adsorption and ion exchange. Amongst these technologies adsorption has recently attracted much attention due to its efficiency, effectiveness and applicability. However, most adsorbents used have high production costs which makes this technology impractical to be widely used. Therefore there is an upsurge of interest in developing low cost adsorbents that will result in low cost adsorption treatment for wastewater, specifically, AMD, since it has become a very significant issue (Singhi et al., 2016). This study focuses on the development of geopolymers using BOFS and FA, and their potential use as sorbents to remediate AMD. The use of BOFS and FA will solve environmental pollution problems associated with their disposal but also help in conservation of natural resources such as limestone and aggregates. Geopolymers have been reported to have high adsorption capacity and providing prolonged alkalinity and may be an effective alternative to commercial alkaline materials, such as lime and sodium hydroxide. Surprisingly few investigations have been conducted regarding the potential of geopolymers for application in remediation of industrial effluents such as AMD (Bajare and Bumanis, 2014; Bumanis et al., 2015; Novais et al., 2016). Limited studies (Al-Zhoon et al., 2011; Mohammad et al., 2015; Andrejkovičová et al., 2016; Duang et al., 2016; Liu et al., 2016; Sarkar et al., 2017) on this new concept have focused on batch experiments using synthetic industrial effluents that are either alkaline or mildly acidic; powdered geopolymers were used instead of geopolymer composites as adsorbents. The aforementioned studies demonstrated that powdered geopolymers can be used as adsorbents to remove metals from wastewater. These studies provided basic knowledge about theoretical removal capacities and kinetics. However, in the treatment of AMD, the presence of competing ions can substantially hinder removal efficiencies. Thus, there is no available

information on the direct application of this method under acid conditions. The present research was conducted using real AMD. To the authors knowledge there is no report in literature that explored or investigated the use of BOFS/FA based geopolymers both as a powder or composite in column studies to remediate AMD; However, Novais et al., 2016 demonstrated that lead adsorption can be achieved using FA based geopolymer composite as an adsorbent; where a maximum lead uptake of 6. 34 $mg_{lead}/g_{geopolymer}$ was achieved. Therefore, geopolymer composites that were developed in this study were used in packed beds, making it easier to collect and recycle them when exhausted (Novais et al., 2016). This is a key practical and beneficial aspect in the real world compared to the use of powdered geopolymers.

Methodology

2.1. Materials and Methods

Acid mine drainage was collected from the Witbank coal mine and its characteristics are shown in table 1. The characteristics of BOFS was obtained from ArcelorMittal South Africa. Fly ash was supplied by Camden power station South Africa. Sodium hydroxide was supplied by Rochelle Chemicals South Africa. Sodium silicate was supplied by Sigma Aldrich. 1000 ppm standards of different metals were diluted accordingly and used as calibration standards for AAS analysis. HCl and HNO_3 were used for sample digestion and preservation.

Table 1. Raw AME characteristics

Parameter		Raw AME	DWAS Guidelines
pH		2.5	>6
Turbidity	(NTU)	547	0-5
EC	(Mv)	240	0-700
Na	(mg/L)	49	0-50
Mg	(mg/L)	27	0-27
Ca	(mg/L)	30	0-32
Fe	(mg/L)	546	0-0.1
Mn	(mg/L)	542	0-0.05

Ni	(mg/L)	390	0-0.07
Al	(mg/L)	344	0-0.9
Cu	(mg/L)	432	0-1
Zn	(mg/L)	364	0-0.5
Cr	(mg/L)	0.054	0-0.01
Pb	(mg/L)	0.9	0-0.01
B	(mg/L)	0.2	0.01
SO_4^{2-}	(mg/L)	3400	0-500

85

86 Table 1 shows the AMD constituents that are present in raw AMD. Raw AME is characterized as
87 highly acidic (pH<3) with high conductivity and turbidity that is way above the stipulated range
88 by DWAS. This was attributed to high levels of Fe, Mn, Ni, Al, Cu, Zn and SO_4^{2-}. Traces of Cr,
89 Pb, B, Ca, Mg and Na were also present. The highly concentrated AMD constituents (Fe, Mn,
90 Ni, Al, Cu, Zn and SO_4^{2}) were chosen as species of concern that are addressed in this paper.
91 Parameters such as turbidity, pH and conductivity were also monitored during the experiments as
92 they are above the range of acceptable limit stipulated by DWAS.

93 **Table 2: Chemical and geotechnical properties of BOFS and Fly Ash**

Parameter	BOFS	FA
pH	12.4	10.79
Specific gravity	3.25	2.42
%Na_2O	0.191	0.905
% CaO	51.81	12.66
% Al_2O_3	3.5	16.07
% SiO_2	7.7	40.4
% MnO	4.188	0.25
% Fe_2O_3	27.58	24.6
% Gravel	0	0
% Sand	77.92	45
% Fine	11.12	55

% Silt	10.96	54.7
%Clay	0	0.4
Liquid limit	76	54
Plastic limit	non plastic	3.65
Shrinkage limit	non shrinking	4.2
MDD (kg/m^3)	2265	1205
OMC (%)	10.58	24.3

94

95 Table 2 shows the BOFS chemical constituents and their compositions respectively. BOFS is
96 mainly composed of calcium oxide (CaO), magnesium oxide (MgO), silicon dioxide (SiO_2), and
97 iron oxide (Fe_2O_3) (Yildrim et al., 2015). It is notable that Fe_2O_3 content in BOFS in this present
98 study is higher compared to those reported in literature. However, it was reported by Shen et al.
99 (2009) that the amount of Fe_2O_3 in BOFS is dependent on the rate of oxidation of excess iron
100 that remained unrecovered during the conversion of molten iron process, and the maximum
101 content that has been reported ranges between 35%-38% (Yildrim et al., 2011). BOFS has the
102 lowest SiO_2, Al_2O_3, Na_2O content compared to other aluminosilicate sources (mine tailings, coal
103 fly ash, metakaolin and granulated blast furnace slag (GBFS)) which have been used to achieve
104 an efficient geopolymer synthesis. SiO_2 and Al_2O_3, contents of BOF slag are respectively 5-7
105 times and 6-8 times lower than those of fly ash, metakaolin and GBFS. In this study the problem
106 of low SiO_2 and Al_2O_3 in BOF slag is addressed through Na_2SiO_4 and fly ash addition. The
107 addition of sodium silicate provides Si^+ ions as a secondary source and the Na^+ ions is an
108 important factor in the geopolymerisation process as it is responsible for balancing charged ions;
109 this also helps to enhance strength development (Part el al., 2015). On the other hand; due to easy
110 availability, alumino–silicate composition, low water demand and high workability of fly ash;
111 Fly ash was used to supplement BOF slag with Si/Al to harness its potential to synthesize a
112 porous hydraulic geopolymer which can be used as a geo-filter to remediate industrial effluents.
113 It is also noticeable that BOF slag compositions are similar to those of clinker. This composition
114 simply reveals that BOF slag exhibits cementitious properties, as has been reported by several
115 researchers that BOF slag is a weak Portland cement clinker (Xie et al., 2012). This is due to the
116 lower content C_3S in BOF slag compared to Portland cement and sometimes the C_3S is not in

the BOF slag sample at all (Tsakiridis et al., 2008). However, the BOF slag sample used in this study reveals that the C_3S is present since the CaO/Si ratio is greater than 2.7 (Shi 2002). The C_3S is well known to be responsible for initial setting, hardening and early strength development of Portland cement concrete (Paria and Yuet., 2006; Reddy et al., 2006). Additionally the high Ca content in BOF slag will play a role to form C-H-S gel during alkaline activation. The C–S–H gel assists in obtaining a dense geopolymer paste resulting in homogeneous products (Singhi et al., 2016; Kumar et al., 2010). It is also well documented in literature that alkaline activation of fly ash using a solution of polysialates forms a cementitious material, consisting of alumino–silicate–hydrate (A–S–H) gel (Kumar et al., 20010; Part et al., 2015;Belhadj et al., 2012). Based on the properties of BOF slag revealed by XRF analysis; this study attempted to investigate the feasibility of synthesizing BOFS/FA based geopolymers via alkaline activation (NaOH solution); to be used as attenuators to decontaminate acidic mineral effluent. In this study AMD was used as a typical stream of Acidic Mineral Effluents.

2.2. Instrumentation

Perspex sheets were supplied by Glass world. An analytical balance (Radweg PS 6000/c/l) was used to weigh the reagents. pH and conductivity were measured using a potentio meter (sension Tm+ pH25+). The concentration of metal in AMD before and after treatment were measured using Atomic absorption spectroscopy (AAS; ICE 3000 series). X-Ray fluorescence (XRF; Rigaku ZSX Primus II) was used to determine the elemental composition of the geopolymer before and after AMD treatment. Malvern Particle Analyser Mastersizer (2000) was used to determine the particle size distribution (PSD) of the geopolymer matrix using the laser diffraction technique. FTIR (Thermo scientific IS10) was used to characterize the geopolymer matrix before and after the experiments. XRD was used to identify the mineralogical phases on the geopolymer before and after treatment. The geopolymer morphology was captured using a Scanning Electron Microscopy (SEM; Tescan Vega 3 XMU 1).

2.3. Synthesis of geopolymers

28.3 g of fly Ash and 254.7 g of BOF slag sample was mixed with 56.6 ml of 5 M NaOH solution and H_2O_2. The H_2O_2 content was varied from 0% to 1.5 %. The obtained paste was then

poured into a 50 × 50 ×50 mm^3 mold. The paste was then allowed to set and harden. The hardened samples were then cured at 80ºC until they were dry. Table 3 shows the densities of BOFS based geopolymers prepared at different H_2O_2 content; 0%, 0.5%, 1% and 1.5% respectively.

Table 3. Densities of BOFS/FA based geopolymers prepared at different H_2O_2 content

H_2O_2 content (%)	0	0.5	1	1.5
Densities (kg/m^3)	2608	2087	1597	1256

2.4. Column tests

Column test experiments were conducted using a Perspex sheet constructed column of 51 mm diameter and 500 mm height. A schematic column test setup is shown in Fig. 1. The geopolymers at different porosities were packed in the columns respectively. The columns were packed with geopolymers prepared with 0%, 0.5%, 1% and 1.5% H_2O_2 respectively. AMD was then percolated through the columns using a fish pond pump. The treated AMD samples were taken from the exit as illustrated in Fig 1. at time intervals 1 day, 3 days, 1 week, a month, 2 months and 3 months. The pH, turbidity and conductivity were also measured. The pH was monitored closely to identify the bed neutralization exhaustion time. All experiments were continued for 133 days until the bed neutralization capacity was exhausted. The treated AMD was subjected to metal concentration analysis using AAS and sulphates were analysed using UV VIS.

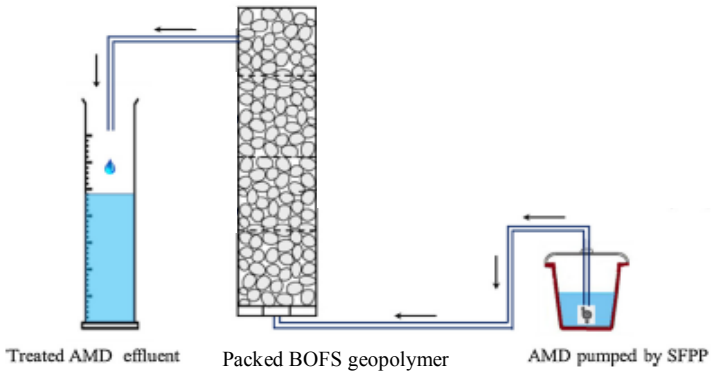

Fig. 1. Schematic diagram of columns tests (Shabalala et al., 2016)

2.5. Open porosity

The specimens were weighed after curing then they were immersed in a water bath for 24 h. 24 h had been determined as the time when an increase in mass of the wet specimen is less than 1%. After 24 h the specimens were removed from water and were wiped using a soft cloth to remove any visible water. The wet specimens were weighed within 5 min after being removed from the water. Open porosity, *f*, was then calculated using equation (1) as follows (ASTM C373 – 14):

$$f = \frac{Ws - Wd}{V\alpha}$$

where *Ws* is the mass of the soaked specimen, *Wd* is the mass of the dry specimen, *V* is the volume of the specimen and α represents the density of water.

2.6. Toxicity Characteristic Leaching Procedure (TCLP)

The leachability of BOFS was determined using an extraction buffer of acetic acid and sodium hydroxide (pH 4.93±0.05) at a liquid/solid ratio of 20:1 (USEPA. 1992). A thermostatic shaker was used for the extraction and the sample was subjected to 24 hours shaking at 25±2ºC. After 24 hours three samples were taken per test conducted and filtered. The leachate was analysed using AAS to determine the concentration of leached metals.

Results and discussion

3.1. The effect of H_2O_2 on the open porosity of BOFS/FA based geopolymer

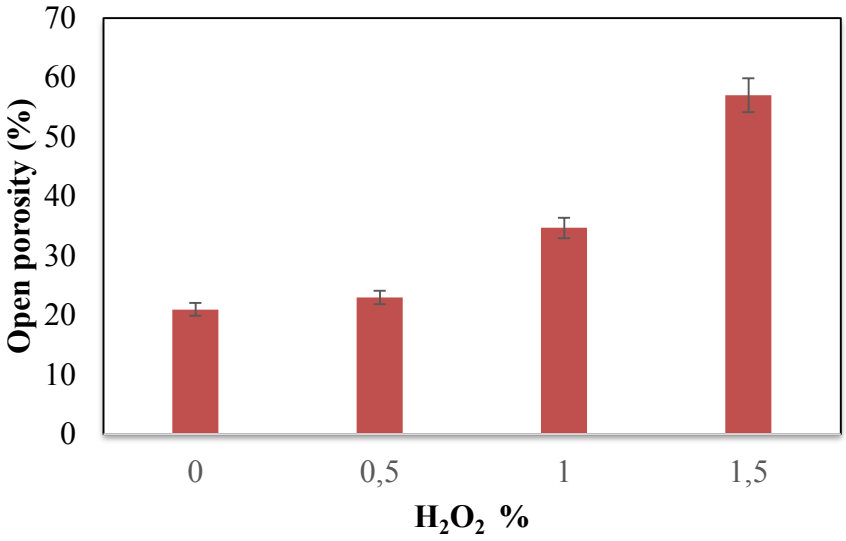

Fig. 2. The effect of H_2O_2 content on open porosity of the geopolymer

Fig. 2 shows that hydrogen peroxide can be used as a blowing agent to increase the porosity of the BOFS based geopolymers. As the H_2O_2 content was increased, the geopolymers became more porous. The open porosity of the geopolymers increased in the following order 1.5%>1%>0.5%>0% with corresponding % of open porosities as follows 21%, 22%, 35% and 57% respectively. Fig 3 shows the geopolymer images at different H_2O_2 content.

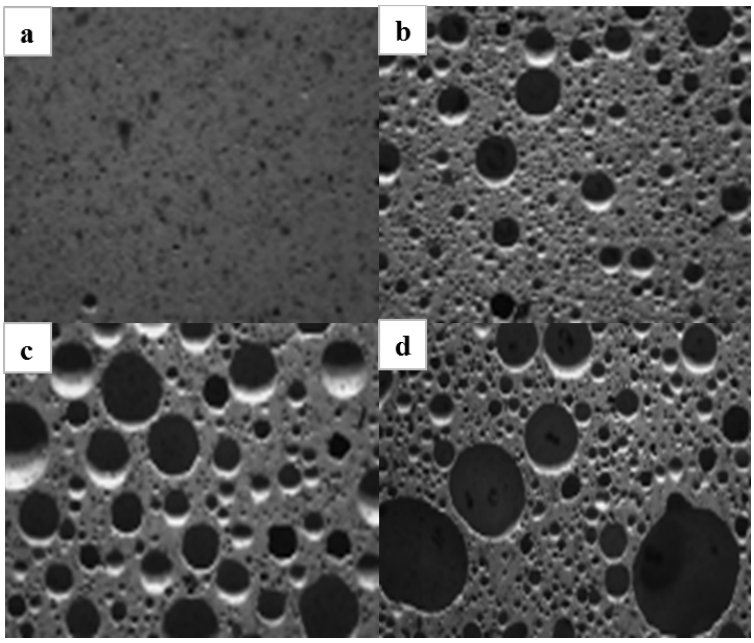

Fig. 3. The effect of H_2O_2 on the BOFS geopolymer composites

Fig. 3. shows the micrographs before (a) and after addition of H_2O_2 (image b, c and d). The b, c and d micrographs represent the addition of 0.5%, 1% and 1.5% H_2O_2 content respectively. The increase in H_2O_2 content resulted in an increase in the number and pores size of the geopolymers.

3.2. The effect of H_2O_2 content on the density and water absorption

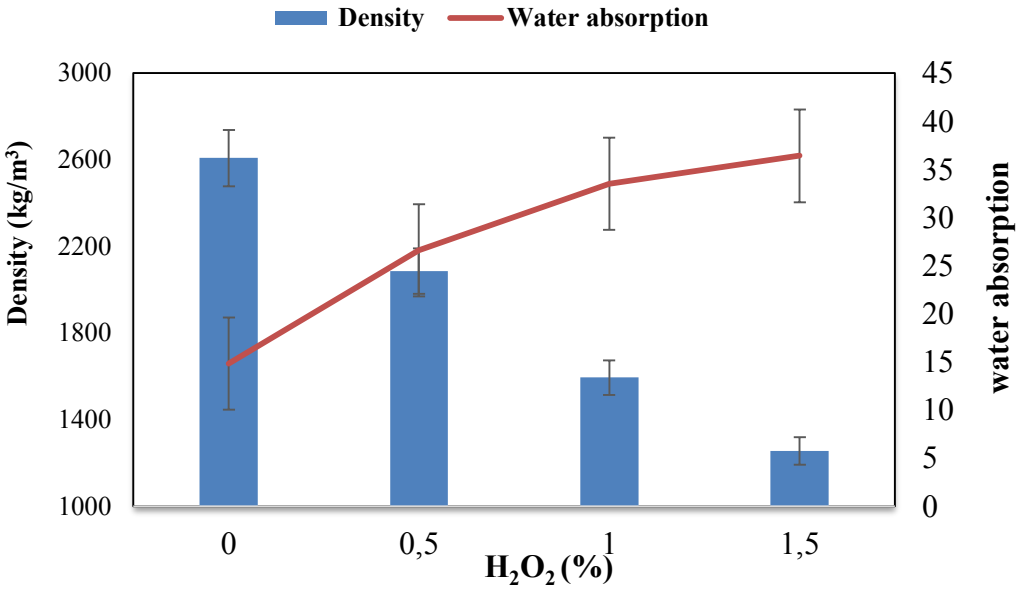

Fig. 4. The effect of H_2O_2 content on the density and water absorption

Fig. 4 shows that as the geopolymers became more porous the water absorption increased while their density decreased. Similar results have been report by (Novais et al., 2016). Low bulk density is associated with high water uptake due to high porosity associated with such composites (Falayi 2016). Low porosity is also associated with high contact between particles hence less water can be absorbed.

3.3. Metals Removal Efficiencies

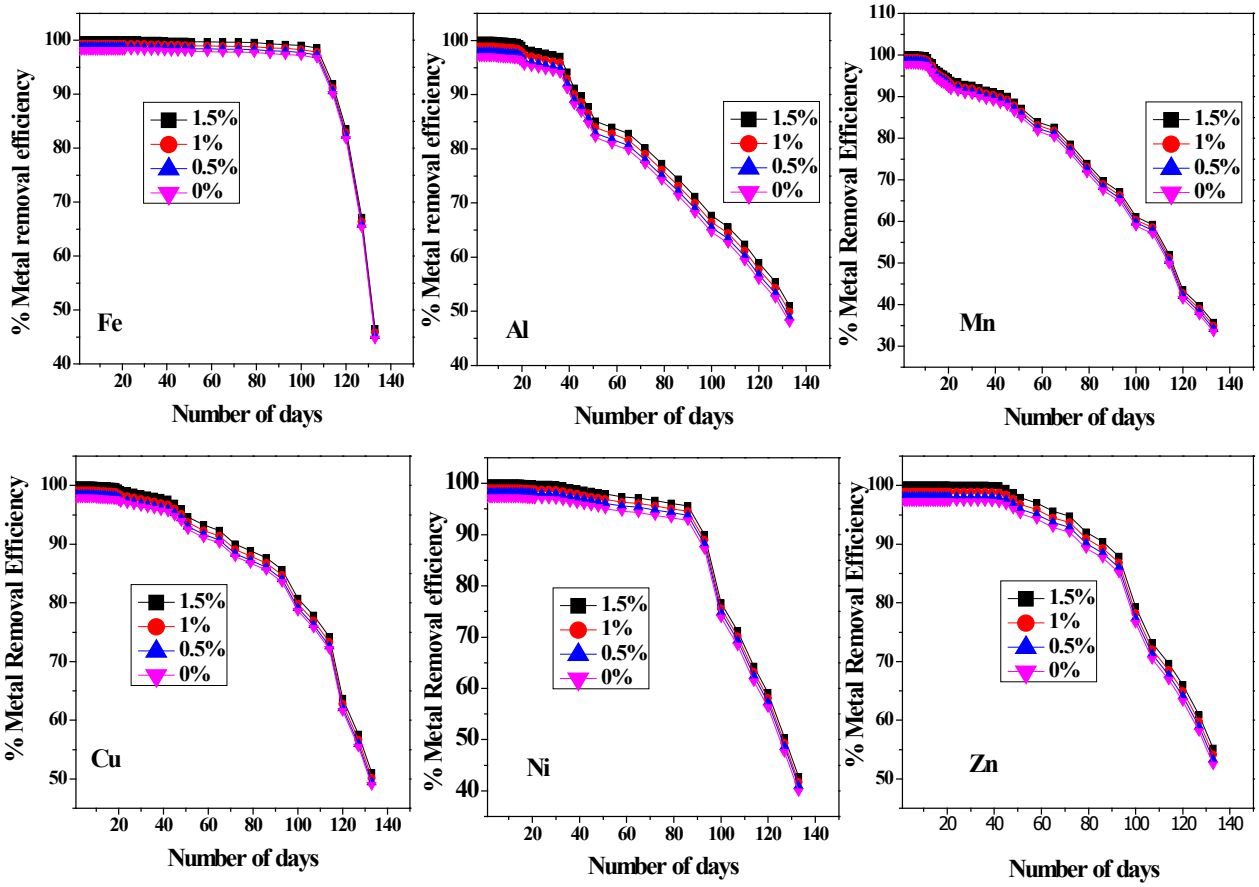

Fig. 5. The effect of variation of H_2O_2 content on the removal of metals

The effect of varying H_2O_2 content on the removal of metals namely; Fe, Al, Mn, Cu, Ni and Zn was studied. The results show that BOFS/FA based geopolymer is very effective in removing the

aforementioned metals. However, the geopolymers effectiveness decrease with continuous reuse of the BOFS/FA based geopolymers. Numerous factors resulted in the decrease in the effectiveness of the geopolymer matrix in all the columns ; (1) the sorption sites are coated by the metals which affects their removal efficiencies; (2) The geopolymer matrix has reached a point of saturation; (3) The AME is no longer neutralized by the geopolymers in the columns. In all the columns regardless of the variation of H_2O_2 content the trend of metal removals were similar, however, Mn removal rate decreased faster as compared to other metals. This is due to the fact that Mn has high affinity and it is greatly affected by competition from other metals hence it is not easily sorbed by the BOFS/FA based geopolymer (Ahmaruzzaman et al., 2011). Although at the beginning of column tests over 99 % Mn removal was achieved. The results also reveal that porosity/ the increase in H_2O_2 content is not the key factor that drives the removal efficiency of the metals; the variation of H_2O_2 content did not have significant effect on metal removal. The column with geopolymers treated with 1.5 % H_2O_2 achieved 100 % removal efficiency of all metals; Fe Al, Mn, Cu, Ni and Zn for a period of 51 days, 18 days, 10 days, 20 days, 30 days and 42 days respectively. Fig 9.2 on the column with geopolymers treated with 1% H_2O_2 shows that there was marginal decrease in % removal efficiency, this column achieved 99% metal removal efficiency, the % metals removal remained constant for a period of 86 days, 48 days, 26 days, 20 days, 45 days and 15 days for Fe Al, Mn, Cu, Ni and Zn respectively. The marginal decrease in removal efficiency might be attributed the reduction in porosity/ H_2O_2 content from 57 % in the column with geopolymers treated with 1.5% H_2O_2 to 45 % in the column with geopolymers treated with 1% H_2O_2. Furthermore there was a 1% decrease in removal efficiency in the early days of column test in the column with geopolymers treated with 0.5 % H_2O_2, 98% metal removals was achieved. This column kept the 98 % metal removal for a period of 86 days, 14 days, 10 days, 21 days, 33 days and 39 days for Fe Al, Mn, Cu, Ni and Zn respectively. The column with geopolymers treated with 0 % H_2O_2 had the least % metals removal efficiencies and the least column to keep the highest % metal removal efficiency for maximum number of days. Cu and Mn showed rapid decrease, while Fe>Ni>Zn>Al showed much steadier decrease, with the trend in the order given. There seems to be some preferential removal which may be linked to the adsorption capacity or pH related precipitation i.e. pH at which minimum solubility is attained.

3.4. Removal of Sulphates

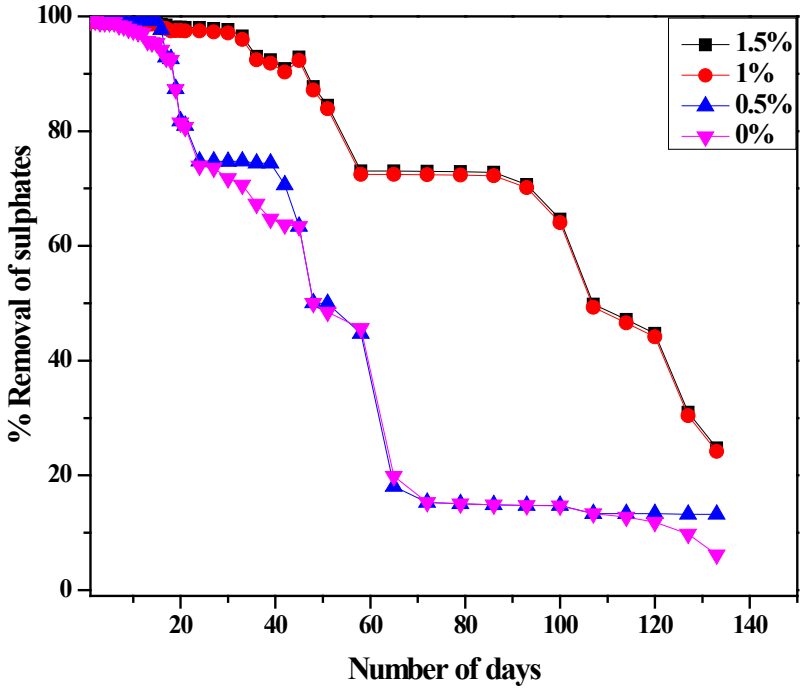

Fig. 6. The effect of variation of H_2O_2 content on the sulphates removal efficiency

Fig. 6 shows the effect of varying porosity/ H_2O_2 content on the sulphates removal efficiency. It can be seen that there was no significant difference in % sulphates removals between the columns packed with geopolymers treated with 1.5% and 1% H_2O_2. Over 99% sulphates removal was achieved by both these columns for a period of approximately 28 days, thereafter there was a decrease in % sulphates removals to 73% in the 62nd day where the % sulphates removals was constant for 30 days before a steady decrease from the 90th day to the 133rd day. The decrease in sulphates removals with number of days indicates that the column packed with geopolymers might have reached their saturation point where they can no longer sorb and scavenge sulphates from AMD for both these columns. Furthermore the column packed with geopolymers treated with 0.5% and 0% H_2O_2 had a marginal % sulphates removal, 99% sulphates removal was achieved from the 1st day to the 18th day, thereafter there was a sharp decrease in % removal from the 18th days to the 31st day. In this region there was a constant removal of sulphates of

72% for the column packed with geopolymers treated with 0.5% H_2O_2 for a period of 19 days thereafter a sharp decrease continued until the 65th day; whilst the column packed with geopolymers treated with 0% H_2O_2 continued to sharply decrease in sulphates removal until the 65th day. From the 66th day the sulphates removals was constant where only 12% of sulphates were removed until the 133rd day for the column packed with geopolymers treated with 0.5 % H_2O_2 whilst the column packed with geopolymers treated 0% H_2O_2 decreased from 12% on the 117th day to below 10 % on the 133rd day. These results demonstrate that porosity/variation of H_2O_2 content influences the sulphates removal, the higher the porosity/ H_2O_2 content the more porous the geopolymer which enhances the effectiveness of the synthesized BOFS/FA based geopolymers.

3.5. pH, conductivity and turbidity

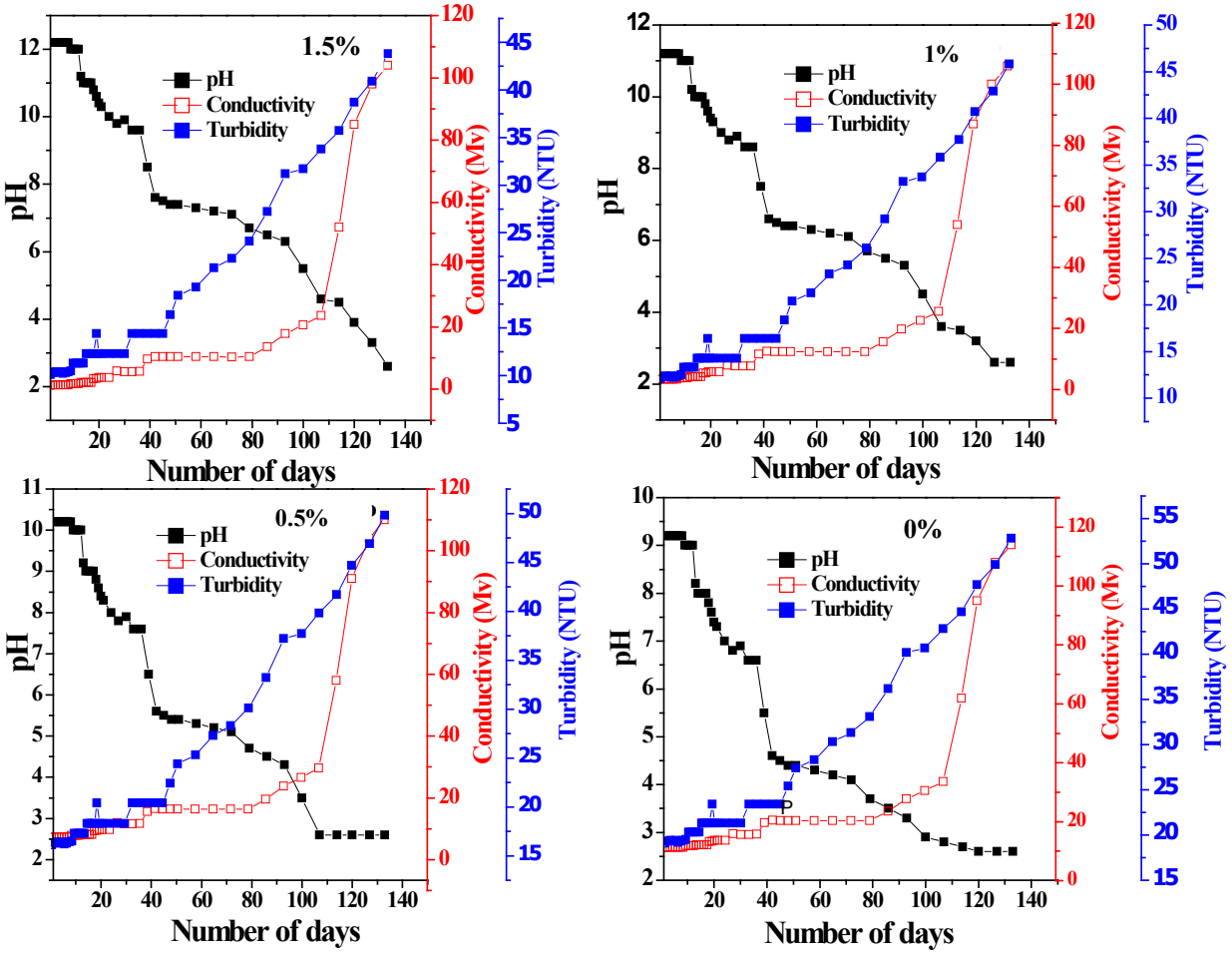

Fig. 7. pH, conductivity and turbidity profiles of geopolymers prepared with different H_2O_2 content over a period of 133 days

Fig. 7 shows the trends between pH, conductivity and turbidity with number of days at different H_2O_2 content. The column packed with geopolymers treated with 1.5% H_2O_2 had the highest pH of 12.2 followed by the column packed with geopolymers treated with 1 % H_2O_2 with pH of 11.2, while the column packed with geopolymers treated with 0.5% H_2O_2 had a pH of 10.3, finally the column packed with geopolymers treated with 0% H_2O_2 had the lowest initial pH of 9.2. These results indicate that the increase in porosity/ H_2O_2 content enhances the extent of the geopolymer alkalinity. In other words the blowing agent H_2O_2 increases the surface area of the neutralization agents/ species in the BOFS/ FA based geopolymer materials which in turn increases the pH of the BOFS/ FA based geopolymer. The pH values suggest that the metals were mainly removed by precipitation as metal hydroxides in the early stages of column tests with sorption as the secondary mechanism of removal. The high pH value in the column packed with geopolymers treated 1.5% column could be used to support the results in Fig. 5 which reported the highest removal efficiency as compared to other columns. The neutralization of the AME was at its highest peak in this column as indicated by the pH and as the pH steadily decreases the removal efficiency also decreases whilst; the turbidity and conductivity gradually increases. The increase in conductivity might reveal that there are cations and anions that remained in solution after AME treatment. The column packed with geopolymers treated with 1 %, 0.5 % and 0 % H_2O_2 followed the same trend as the column packed with geopolymers treated with 1.5% H_2O_2 the only differences was the rate of increase of turbidity and conductivity was high in the following order 0%>0.5%>1%. The order reveals that as the porosity is decreased the higher the conductivity, which indicates that cation and anions remained longer in solution with an increase in number of days. As the geopolymer is being reused the accessible sites become inadequate to neutralize and remove metal and sulphates in AME. The general trend, shown in all the graphs revealed that as the geopolymers are reused for 133 days there was a decrease in pH with an increase in turbidity and conductivity. The increase in redox potential might also be a contributing factor that resulted in a decrease in pH with number of days. As the experiments were conducted for a period of 133 day, the environment might have become more oxidative; increasing the redox potential of the system leading to the release of the precipitated and adsorbed metals into solution, dissolution of sulphate based precipitates and decrease in pH,

reducing the removal efficiencies of metals and sulphates (Popenda 2014). The turbidity and conductivity were at their highest peak on the 133rd day, this conductivity signifies that a large proportion of ions remained in solution without being sorbed by the geopolymers. The increase in turbidity may be due to precipitated ions. Initially these may be trapped in the pores of the geopolymer matrix but may later be washed out of the column increasing turbidity. The decrease in pH with number of days might also be due to redox potential increase resulted from oxidative environment

3.6. XRD analysis of BOFS/FA based geopolymer before and after AME treatment

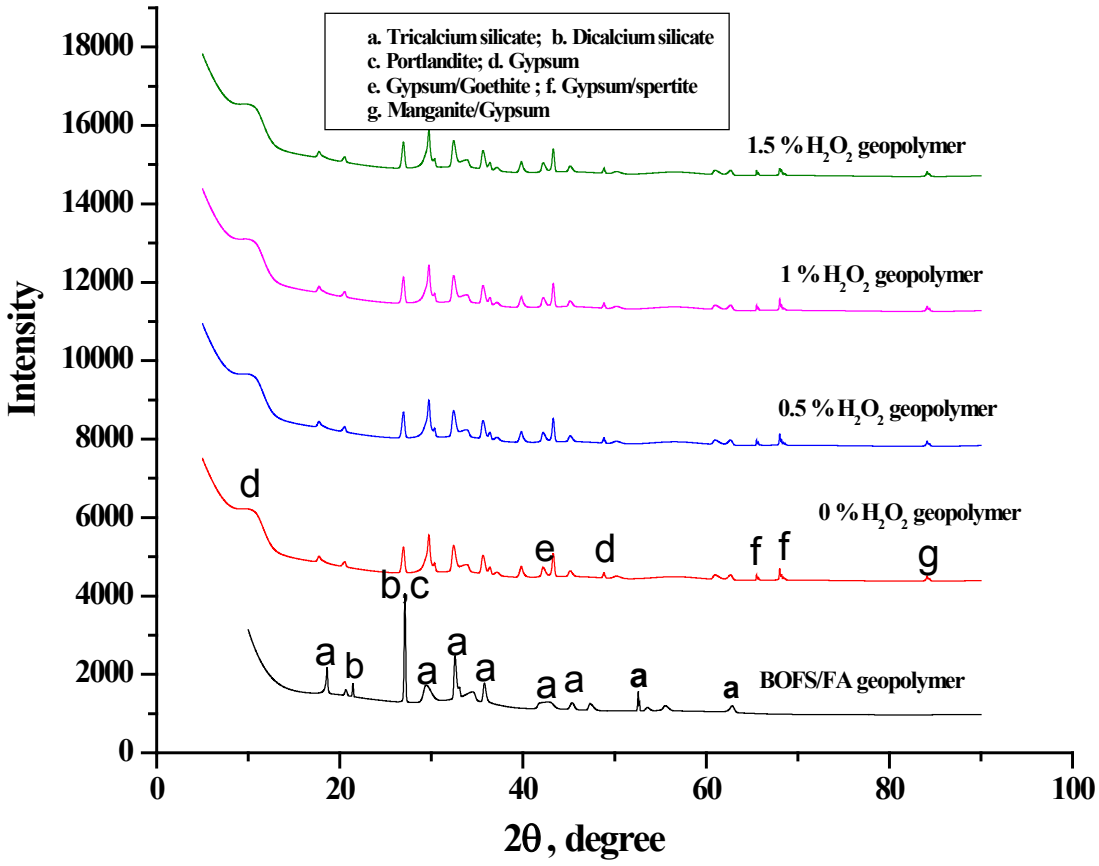

Fig. 8. The XRD pattern of BOFS/FA based at different H_2O_2 content before and after AMD treatment.

The XRD pattern of raw BOFS/FA based geopolymer and the resulting XRD patterns after AMD treatment at different H_2O_2 content is shown in Fig 8. The reference sample BOFS/FA based geopolymer consists of silicates namely tricalcium silicate and dicalcium silicate and portlandite as major mineral phases. However, after AMD treatment the intensity of the tricalcium and dicalcium silicates peaks decrease meaning that the silicates reacted with AMD through ion exchange as shown in Eqn 1-5 resulting in elevation of pH and accumulation of alkalinity which in turn favors the removal of metals by precipitation.

$$CaO + H_2O = CaOH \quad (1)$$

$$3Ca(OH)_2\,(aq) + 3M(SO_4)\,(aq) = 3CaSO_4\,(s) + 3M(OH)_2\,(s) \quad (2)$$

Where M = Mn, Al , Ni, Zn, Fe and Cu

$$\equiv SiOH \leftrightarrow SiO^- + H^+ \quad (3)$$

$$\equiv SiOH + Ca^{2+} \leftrightarrow SiOCa + H^+ \quad (4)$$

$$\equiv SiOCa/Mg + Me^+ + 2HOH \rightarrow =SiOM + Mg/Ca^{2+} + 2OH^- \quad (5)$$

The CaO reacts with H_2O to form a precipitate porlandite as shown in Eqn 1, thereafter porlandite (CaOH) react with metal sulphates as shown in Eqn 2 to form crystalline gypsum and metal hydroxide. Eqn 3 to 5 shows that the silica in fly ash and BOFS might be another parameter, which contributed to in the removal of metals (Masindi et al., 2016). Furthermore, the portlandite peak also decreased because porlandite reacted with metal sulphates as shown in Eqn 2 to form crystalline gypsum and metal hydroxide. It is also noticeable that there was a slight development of a peak at 10° in the resulting geopolymer after AMD treatment that suggests that there is a new mineral phase (gypsum forming). There was also new mineral phases formed at 68.5°, 84° and 43° namely; gypsum and spertiniite and gypsum and manganite, gypsum and goethite respectively. These new mineral phases reveal the gypsum with a content above 80% is the new major phase in the resulting geopolymer after AME treatment; whilst other new phases are considered to be minor suggesting that the metals in AME are predominately removed via precipitation mechanism. Therefore this XRD diffactogram supports the results and discussions in 3.5.

3.7. The IR spectra of BOFS/FA based geopolymers before and after AME treatment

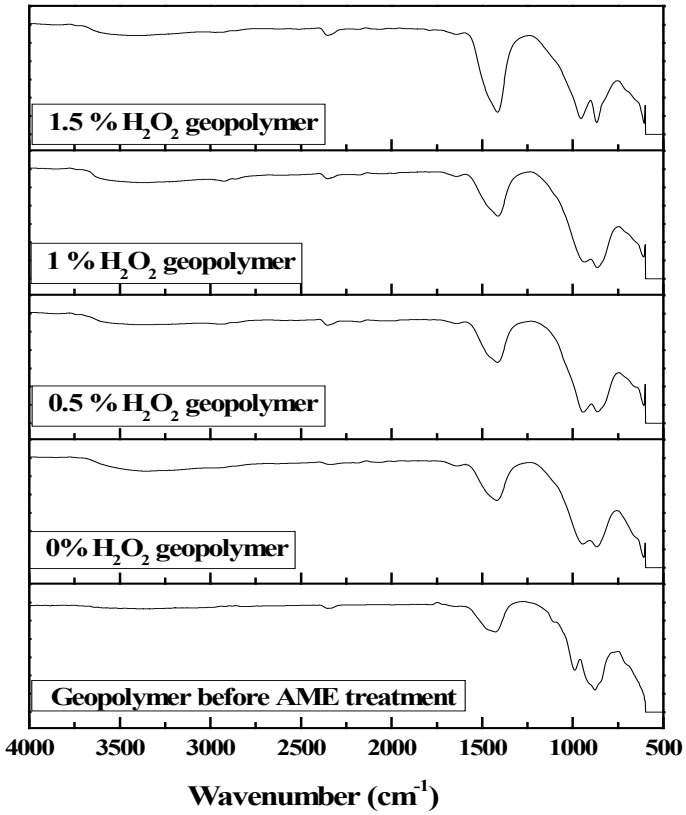

Fig. 9 **The IR spectra of BOFS/FA based geopolymer before and after AME treatment**

Fig. 9. shows the IR spectra of BOFS/FA based geopolymer before and after AME treatment. The mechanisms of metals removal are mainly governed by precipitation and co-precipitation whilst ion exchange and sorption also contributes to a lower extent. The IR structures show that there are precipitates in the resulting geopolymers however, the precipitation of other metals namely; Zn-OH, Mn-OH, Ni-OH and Fe-OH was not confirmed by the IR spectra which were expected to appear with intense bands at 1382cm^{-1}, 15550-1850 cm^{-1}, 600 cm^{-1} and 3360 cm^{-1} respectively.

3.8. Morphology of the BOFS/FA geopolymers before and after AME treatment

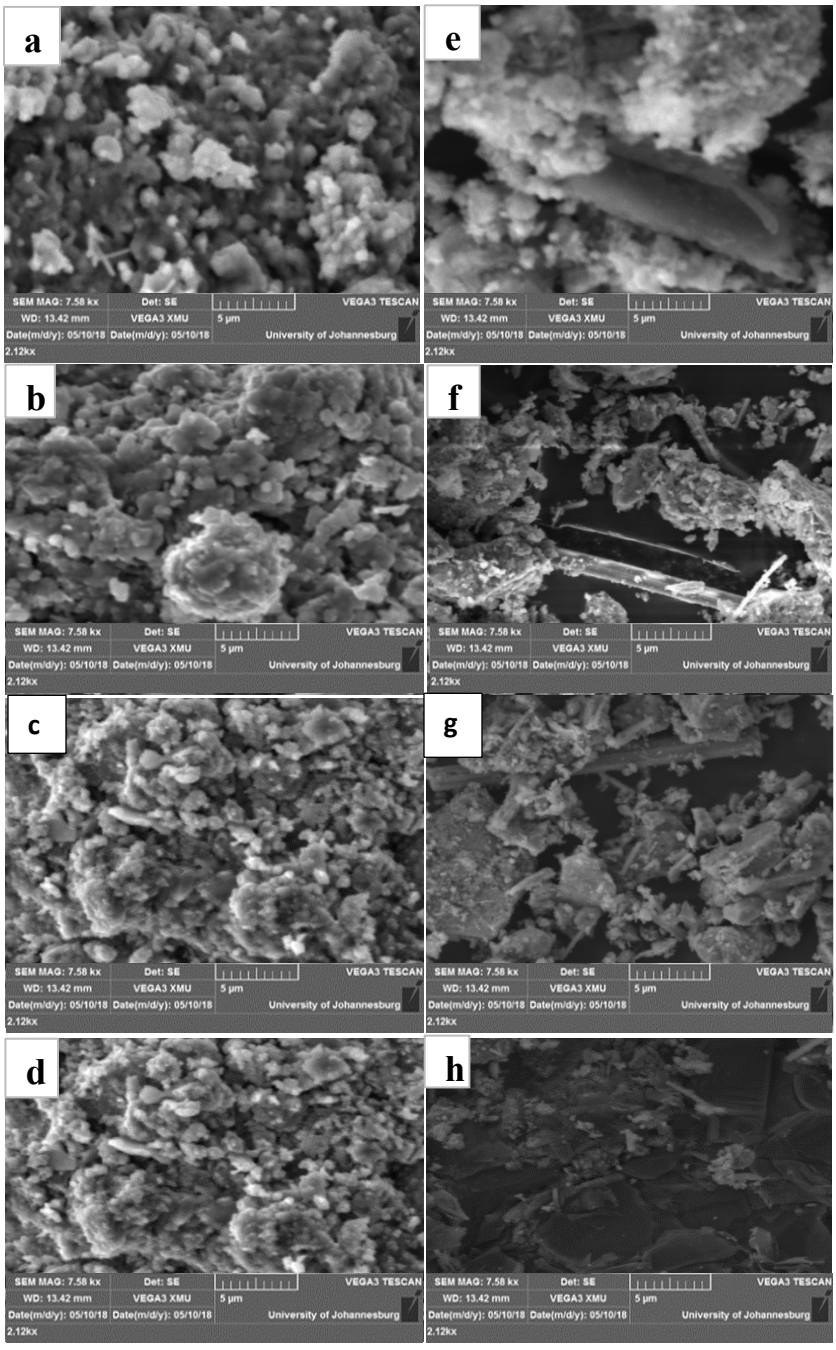

Fig. 10. The SEM micrographs of BOFS/FA geopolymer before and after AME treatment.

406 Fig. 10 shows the SEM micrographs of BOFS/FA based geopolymer before and after treatment.
407 Before AMD treatment the geopolymer particles were spherical, closely packed and dense (a, b,
408 c and d). After AMD treatment the geopolymer residual appeared needle like, with fibrous and
409 rod shaped structure forming on a flat crystal structure indicating the formation of metal and
410 sulphate complexes. The complexes are as a result of coated precipitates and gypsum on the
411 surface of the geopolymer through a physical process.

412 ### 3.9. Toxicity Characteristic Leaching Procedure (TCLP)

413

414 Table 4 shows the leachability of metals from BOFS/FA before and after geopolymerisation.

415 **Table** 4. **TCLP of BOFS/FA before and after geopolymerisation**

Constituents	**Concentration (mg/L**		**USEPA maximum allowed concentration in leachate (mg/L)**
	Raw BOFS/FA	BOFS based geopolymer after AMD treatment	
Arsenic	0.003	0.001	5
Barium	0.923	0.851	100
Cadmium	0.019	0.01	1
Chromium	0.038	0.021	5
Lead	0.005	0.003	5
Mercury	0.015	0.01	0.2
Selenium	0.102	0.09	1
Silver	0.02	0.009	0.1

416

417 Table 4 shows the TLCP results of BOFS before and after geopolymerisation. The
418 geopolymerisation of BOFS resulted in reduction of metals leaching from BOFS. This is due to
419 the presence of zeolite as shown in Fig 8 and Fig. 10. This is also evidence that
420 geopolymerisation resulted in a very tight bond between metals that are not released from the
421 geopolymer matrix. The TCLP analysis results did not exceed the leaching thresholds as
422 stipulated by U.S. EPA standards.

4. Conclusion

BOFS/FA based geopolymers can be used to remove metals and sulphates and neutralize AMD. All the BOFS/FA based geopolymers at different porosities were effective however, the BOFS/FA geopolymers prepared with 1.5% H_2O_2 outperformed the geopolymers prepared/ treated with 0%, 0.5% and 1% in terms of AMD neutralization longevity. The geopolymers prepared/treated with 1.5% H_2O_2 managed to neutralize AMD for over a period of 60 days at a flow rate of 6 ml/min. Characterization revealed that precipitation was the main mechanism for removal of metals. Gypsum was the main byproduct formed with precipitated metals presented by goethite, spertite and manganite.

Acknowledgements

The authors would also like to thank ArcelorMittal (South Africa) for providing the BOFS, Eskom (South Africa) for providing the fly ash and the National Research Foundation (South Africa) for providing financial assistance to conduct this work.

References

Ahmaruzzaman, M., 2011. Industrial wastes as low-cost potential adsorbents for the treatment of wastewater laden with heavy metals. Advances in colloid and interface science, 166(1-2), pp.36-59.

Al-Harahsheh, M.S., Al Zboon, K., Al-Makhadmeh, L., Hararah, M. and Mahasneh, M., 2015. Fly ash based geopolymer for heavy metal removal: A case study on copper removal. Journal of Environmental Chemical Engineering, 3(3), pp.1669-1677.

Al-Zboon, K., Al-Harahsheh, M.S. and Hani, F.B., 2011. Fly ash-based geopolymer for Pb removal from aqueous solution. Journal of hazardous materials, 188(1-3), pp.414-421.

Cheng, T.W., Lee, M.L., Ko, M.S., Ueng, T.H. and Yang, S.F., 2012. The heavy metal adsorption characteristics on metakaolin-based geopolymer. Applied Clay Science, 56, pp.90-96.

Duan, P., Yan, C., Zhou, W. and Ren, D., 2016. Development of fly ash and iron ore tailing based porous geopolymer for removal of Cu (II) from wastewater. Ceramics International, 42(12), pp.13507-13518.

Fernández-López, J.A., Angosto, J.M. and Avilés, M.D., 2014. Biosorption of hexavalent chromium from aqueous medium with opuntia biomass. The Scientific World Journal, 2014.

Gitari, M.W., Petrik, L.F., Etchebers, O., Key, D.L., Iwuoha, E. and Okujeni, C., 2006. Treatment of acid mine drainage with fly ash: removal of major contaminants and trace elements. Journal of Environmental Science and Health Part A, 41(8), pp.1729-1747.

Liu, Y., Yan, C., Zhang, Z., Wang, H., Zhou, S. and Zhou, W., 2016. A comparative study on fly ash, geopolymer and faujasite block for Pb removal from aqueous solution. Fuel, 185, pp.181-189.

Masindi, V., Gitari, M.W., Tutu, H. and De Beer, M., 2016. Fate of inorganic contaminants post treatment of acid mine drainage by cryptocrystalline magnesite: complimenting experimental results with a geochemical model. Journal of Environmental Chemical Engineering, 4(4), pp.4846-4856.

Miretzky, P. and Cirelli, A.F., 2009. Hg (II) removal from water by chitosan and chitosan derivatives: a review. Journal of hazardous materials, 167(1-3), pp.10-23.

Novais, R.M., Buruberri, L.H., Seabra, M.P. and Labrincha, J.A., 2016. Novel porous fly-ash containing geopolymer monoliths for lead adsorption from wastewaters. Journal of hazardous materials, 318, pp.631-640.

Popenda, A., 2014. Effect of redox potential on heavy metals and As behavior in dredged sediments. Desalination and Water Treatment, 52(19-21), pp.3918-3927.

Sarkar, C., Basu, J.K. and Samanta, A.N., 2017. Removal of Ni2+ ion from waste water by Geopolymeric Adsorbent derived from LD Slag. Journal of water process engineering, 17, pp.237-244.

Shabalala, A.N., Ekolu, S.O., Diop, S. and Solomon, F., 2017. Pervious concrete reactive barrier for removal of heavy metals from acid mine drainage− column study. Journal of hazardous materials, 323, pp.641-653.

M.R. Abdi, Effects of basic Oxygen steel slag (BOS) on strength and durability of kaolinite. International Journal of Civil Engineering, 9(2)(2011) 81-89.

M.J.K. Ahmed and M. Ahmaruzzaman, A review on potential usage of industrial waste materials for binding heavy metal ions from aqueous solutions. Journal of Water Process Engineering, 10(2016) 39-47.

S.D. Venmyn, Acid mine water drainage has the potential to become a major issue for South African industry, 2013. Deloitte, Environmental Services and Sabatha Kolver, Mining Weekly Magazine.